Research Paper   Open Access

Transient Pressure Analysis of Horizontal Wells in a Multi-Boundary System

S. Al Rbeawi and D.Tiab,
SPE, University of Oklahoma

Abstract: Horizontal wells can greatly increase the contact area of the wellbore and the pay zone; so they are commonly applied in oil reservoirs to enhance the production and ultimate recovery of oil and gas, especially, in low permeability formations. The purpose of this study is to develop a technique for the interpretation of transient pressure based on dimensionless pressure and pressure derivative. Type curve matching is one of the techniques that can be used to interpret the pressure data of horizontal wells in finite reservoirs. Starting from very short horizontal wells to extra-long wells, the pressure behavior of the wells has been analyzed for different conditions. The effect of the outer boundaries of the reservoir on the pressure behavior of the horizontal wells has been investigated for different configurations. Rectangular shape reservoirs with different dimensions have been used to study the pressure response in the well. Five flow regimes have been observed for regular length horizontal wells; early radial, early linear flow, pseudo radial flow, channel flow or late linear flow, and pseudo-steady state flow. Four flow regimes have been observed for the extra-long wells: linear flow, pseudo radial flow, channel flow, and pseudo-steady state or boundary-affected flow. Of course, those flow regimes do not always take place under all conditions. Pseudo-steady state flow is expected to occur after long production time. A pressure drawdown test was solved using the proposed type curve matching technique. The study has shown that the effect of the boundary on the pressure response of the horizontal wells and the type of flow regimes depend on the length of the horizontal wells and the distance to the nearest boundary**.**

I.   INTRODUCTION

The use of horizontal wells for producing oil and gas from low-permeability and unconventional reservoirs is now very well established within the petroleum industry. The great increase of the surface area of the wellbore that allows fluids to freely flow from the reservoir to the wellbore is the main advantage of the horizontal well. Reducing the effects of the damaged zones and increasing the well deliverability are the direct impacts of this type of increment. Therefore, over the last two decades the number of horizontal wells that have been drilled worldwide has considerably increased due to the possibility of improving the well productivity and anticipating oil and gas recovery. Low-permeability and unconventional reservoirs are not the only common applications for horizontal wells. They also have been used successfully in fractured reservoirs: (a) to intersect natural fractures and effectively drain the reservoir; (b) in water and gas driven reservoirs to minimize water and gas coning; (c) in both low and high permeability gas reservoirs to reduce the number of producing wells; (d) in tertiary recovery application to enhance the contact between the well and the reservoir; and (e) finally, in offshore reservoirs, as well as in environmentally sensitive areas, to cut down the cost of drilling and the number of production facilities. Although, since the mid 1980s, horizontal well technology has provided the solutions for oil and gas production process where the conventional vertical technique either has failed or produced less than the desired rate, the rapid increase in the application of this technology during this period led to a sudden need for the development of analytical models that are capable of evaluating the performance of these horizontal wells. Giger, F. (1985) and Joshi, S. D. (1986) presented the applicability of horizontal wells in heterogeneous reservoirs and the impact of the well productivity using slanted or horizontal wells respectively. Spivak, D. (1988) explained that the advantages of horizontal wells, such as producvtivity increase, better sweep efficiency, and reduction of water and gas coning, have been reported by many researchers. At the same time, many researchers, such as Babu, D. K. and Odeh, A. S. (1989) and Goode, P. A. and kuchuk, F. J. (1991), have attempted to develop practical models to study the performance and productivity of horizontal wells.Over time, transient pressure analysis techniques have been favorably applied for the evaluation of horizontal well performance and reservoir characterization. Daviau et al (1988) presented solutions using the Newman product

method for an infinite limited isotropic reservoir as well as for an isotropic reservoir with constant pressure at the outer boundaries. Clonts, M.D. and Ramey, H. J. (1986) developed one of the earliest analytical models for horizontal well test analysis based on the line source approximation of the partially penetrating vertical fracture solution. Ozkan et al (1989) have shown the effect of the producing length of horizontal wells on the pressure derivative response. Carvalho, R.S. and Rosa, A.J. (1989) introduced a mathematical model for pressure evaluation in infinite conductivity horizontal wells. Odeh, A.S. and Babu, D.K. (1990) studied the transient flow behavior for horizontal wells for both pressure drawdown and pressure build-up tests. Because of the increased complexity in the geometrical configuration of the wellbore as a result of the different horizontal well completion techniques, many concerns and limitations regarding the pressure behavior in the vicinity of the wellbore and outer no-flow boundaries have remained unanswered. These concerns are based on the fact that the ideal behavior is hardly ever seen in real production tests because the pressure derivative can exhibit very different trends depending on the geometrical configuration of the whole system, the petrophysical properties of the formation, and zonal damage. Therefore, the validity of the horizontal well models and the well test concepts adopted from vertical fracture analogues have been extensively investigated and new trends of horizontal well solutions were developed in the beginning of the 1990s. These solutions have been established under more realistic conditions to provide the answers for previous concern and limitations. Kuchuk et al (1991) studied the effect of the presence of the gas cup or aquifer on the pressure transient behavior of horizontal wells. Guo, G. and Evans, R. D. (1993) presented an analytical model for the pressure transient behavior and inflow performance of horizontal wells intersecting discrete fractures. Automatic type curve matching for horizontal wells has been introduced by Thompson, L.G. and Temng, K.O. (1993). Ozkan et al (1995) studied the effect of conductivity on transient pressure response of horizontal wells. Economides et al 1996 presented the effects of the well configurations on pressure behavior and well productivity for horizontal wells acting in anisotropic formation. They also introduced new methodology for horizontal plane shape factor determination. Verga et al (2001) investigated the transient dual-porosity pressure response of two horizontal wells and introduced numerical models to reproduce the reservoir internal geometry and simulate the pressure trend monitored at the wells. Khelifa and Taib (2002) proposed a technique for analyzing the variable rate tests in horizontal wells by using continuously changing flow rate test or by using a series of constant rate test. Hashemi et al (2004) demonstrated how the horizontal well flow regimes are affected by condensate accumulation and how this modifies the pressure derivative shapes. It is important to note that Escobar et al (2004) have used the TDS technique to analyze the pressure behavior of a horizontal well inside a channel system. A physically consistent model for describing transient pressure behavior of horizontal drainholes was established by Ogunsanya et al (2005) to overcome the basic limitations in previous models. The last ten years has seen a focus on using the convolution and deconvolution technique in well test analysis. Von Shorter et al (2001) showed that the use of deconvolution of well test data is a nonlinear total least squares problem. Gringarten et al (2003) proposed the use of downhole pressure gauges to diagnose production problems in North Sea horizontal wells. Ilk et al (2005) studied using B-spline deconvolution of variable rate reservoir performance data. Whittle et al (2009) introduced a technique for well production forecasting by extrapolation of the deconvolution of pressure transient data. Gringarten, A. C. (2010) explained the practical use of the well test convolution and the various usages of deconvolution in tests of short and long durations. Even though great attention has been focused on horizontal well technology either in the drilling and completion aspect or in the production and reservoir characterization aspect, more study is required to overcome the concerns and limitations of the models that are used to evaluate the performance of wells or to predict the pressure behavior around and in the wellbore. This fact is supported by the idea of the great complexity of the horizontal well system and the difficulties that are governing the recognitions of the flow dynamics and types of flow regimes especially in the area near the well where the geometrical configuration of flow becomes of great importance. In this paper a technique for the interpretation of transient pressure based on dimensionless pressure and pressure derivative is introduced. This technique depends on the results obtained from an analytical model for a horizontal well acting in finite reservoir having a rectangular shape. A set of type curve matching plots for the wells is established for very short horizontal wells and extra-long wells taking into account the change in either the distance to the outer boundaries in the two directions or the length of the producing horizontal section. The study includes the effect of the outer boundaries of the reservoir on the pressure behavior of the horizontal wells.

Horizontal well in an infinite reservoir

Consider a horizontal well, such as in Fig. (1), producing slightly compressible petroleum fluids from an infinite-acting reservoir at a constant rate. To simulate the transient pressure response of this well, an analytical model should be used for this purpose. The following assumptions are very important for the selection of this model:

1- The reservoir is homogenous and having constant and uniform thickness with two impermeable layers at the top and bottom of the formation.

2- Constant porosity and permeability in each direction, but the formation is anisotropic.
3- Gravitational and frictional effects are negligible.
4- No-flow boundaries.

The solution to the diffusivity equation based on the above conditions can be obtained using different techniques which are applicable for the transient flow of fluid in the porous media. Gringarten, A. C. and Ramey, H. J. (1973) were the first to introduce the use of the source and Green's function in solving unsteady state flow problems in the reservoirs. They stated that the infinite line source can be visualized as the intersection of two perpendicular infinite plane sources normal to two of the three principal axes of permeability while the point source can be visualized as the intersection of three perpendicular infinite plane sources normal to the principal axes of permeability. Ozkan, E. (1988) introduced new source solutions to the diffusivity equation using the Laplace space to overcome the difficulties that might result when we apply the Grinarten and Ramey's source solution in complex geometrical configurations such as dual-porosity and dual-permeability porous media. Spivak, D. (1988) presented the same solution considering the infinite line source as a result of the integrating process for any point from $(-\infty$ to $+\infty)$ and the pressure drop distribution created by a continuous source of any shape can be obtained by the principal of the superposition in time and space. Therefore a line or a plane source can be generated by superposing an infinite number of point source along the line or plane.

The mathematical model can be used to simulate the pressure behavior created by the constant production of a horizontal well having a known length $(2L_w)$ and extending in the midpoint of an infinite formation having a known height (h) is (Daviau et al 1988):
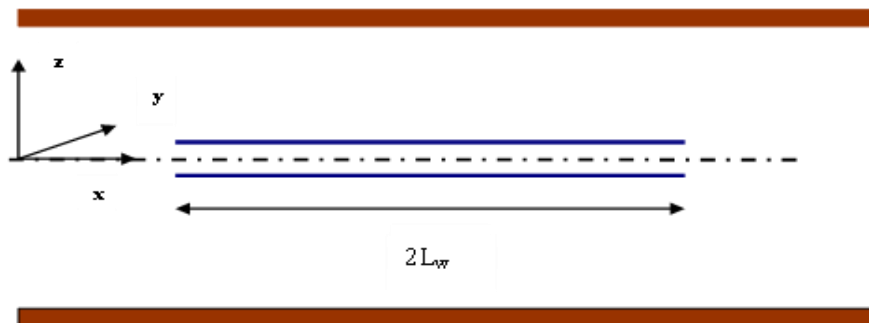
Figure 1: Horizontal well acting in an infinite reservoir.

$$P_D(x_D, y_D, z_D, z_{wD}, L_D, t_D) = \frac{\sqrt{\pi}}{4} \int_0^{t_D} \frac{e^{-\frac{y_D^2}{4t_D}}}{\sqrt{\tau_D}} \left[erf(\frac{1+x_D}{2\sqrt{\tau_D}}) + erf(\frac{1-x_D}{2\sqrt{\tau_D}}) \right] \times$$

$$\left[1 + 2\sum_{n=1}^{\infty} \exp\left(-n^2\pi^2 L_D^2 \tau_D\right) \cos(n\pi z_{wD}) \cos(n\pi(\bar{z}_D + z_{wD})) \right] d\tau_D \qquad (1)$$

where the dimensionless parameters in the above model are defined as follows:

$$x_D = \frac{x - x_w}{L_w} \qquad (2)$$

$$y_D = \frac{y - y_w}{L_w} \sqrt{\frac{k_x}{k_y}} \qquad (3)$$

$$z_D = \frac{z - z_w}{L_w} \sqrt{\frac{k_x}{k_z}} \qquad (4)$$

$$z_{wD} = \frac{z_w}{h} \qquad (5)$$

$$\bar{z}_D = \frac{z - z_w}{h} = z_D L_D \qquad (6)$$

$$L_D = \frac{L_w}{h}\sqrt{\frac{k_z}{k_x}} \tag{7}$$

$$t_D = \frac{k_x t}{\phi \mu c_t L_w^2} = \frac{\eta_x t}{L_w^2}, \quad \text{where } \eta_x = \frac{k_x}{\phi \mu c_t} \tag{8}$$

$$P_D(x_D, y_D, z_D, z_{wD}, L_D, t_D) = \frac{2\pi\sqrt{k_x k_y}\,h\Delta P}{q\mu} \tag{9}$$

and:

$$Q = \frac{q}{2L_w} \tag{10}$$

It is clear that the above model consists of three instantaneous source functions which are S(x, t), S(y, t), and S(z, t).   S(x, t) represents the infinite slab source in an infinite reservoir and S(y, t) represents the infinite plane source in an infinite reservoir while S(z, t) represents the infinite plane source in an infinite slab reservoir. To solve the above model, two approximations should be done for the three functions based on the fluid flow dynamic and flow regimes in early and late time.

Short-time approximation
At early time, it is known that there is no flow in the reservoir beyond the tips of the well. Therefore short-time approximation can be obtained by considering the asymptotic behavior of the three instantaneous source functions that are involved in the model. The first instantaneous function S(x, t) =1 when the monitoring point is located inside the well as the time approaches zero (Spivak 1988):

$$S(x_D, t_D) = \frac{1}{2\sqrt{\pi\eta_x t}} e^{-\frac{(x-x_w)^2}{4\eta_x t}} = 1 \tag{11}$$

and the proper time limit for the above equation to be applied as determined by Gringarten and Ramey (1973) is:

$$t_D = \frac{(1-x_D)^2}{20} \tag{12}$$

The second instantaneous function S(z, t) has the following formula:

$$S(z_D, t_D) = \frac{1}{2\sqrt{\pi\eta_z t}} e^{-\frac{(z-z_w)^2}{4\eta_z t}} = \frac{1}{2\sqrt{\pi t_D}L_w}\sqrt{\frac{k_x}{k_z}} e^{-\frac{z_D^2}{4t_D}} \tag{13}$$

Since this function deals with the infinite plane source in an infinite slab reservoir, there is a time at which the upper or lower boundary starts to affect the pressure behavior. This time can be estimated by:

$$t_D \leq \min\left[\begin{array}{c}\frac{[(\bar{z}_D + 2z_{wD})/L_D]^2}{20} \\ \frac{[(\bar{z}_D + 2z_{wD} - 2)/L_D]^2}{20}\end{array}\right] \tag{14}$$

while the third instantaneous function S(y, t) has the following formula for the short time approximation:

$$S(y_D, t_D) = \frac{1}{2\sqrt{\pi\eta_y t}} e^{-\frac{(y-y_w)}{4\eta_y t}} = \frac{1}{2\sqrt{\pi t_D}L_w}\sqrt{\frac{\eta_x}{\eta_y}} e^{-\frac{y_D^2}{4t_D}} \tag{15}$$

and the proper time for this approximation to be applicable is:

$$t_D = \frac{y_D^2}{20} \tag{16}$$

Based on the short time approximations for the above three functions, the short time approximation for Eq. (1) can be written as the product of the three approximations:

$$P_D(x_D, y_D, z_D, z_{wD}, L_D, t_D) = \frac{1}{4L_D} \int_0^{t_D} \frac{1}{\tau_D} e^{-\frac{\left[y_D^2 + z_D^2\right]}{4\tau_D}} d\tau_D = -\frac{1}{4L_D} Ei\left(-\frac{y_D^2 + z_D^2}{4t_D}\right)$$

$$= \frac{1}{4L_D}\left(\ln\left(\frac{t_D}{y_D^2 + z_D^2}\right) + 0.80907\right) when \ Ei\left(-\frac{y_D^2 + z_D^2}{4t_D}\right) \le 0.01 \tag{17}$$

Long-time approximation

At late time, the pressure behavior of horizontal wells starts to be affected by the pseudo-steady state flow. Therefore the long time approximation of Eq. (1) takes into consideration this fact. The first instantaneous function which represents the infinite slab source in an infinite reservoir is approximated as follows (Spivak 1988):

$$S(x_D, t_D) = \frac{1}{2\sqrt{\pi \eta_x t}} e^{-\frac{(x - x_w)}{4\eta_x t}} = \frac{1}{\sqrt{\pi t_D}} \tag{18}$$

and the long limit of the time so that the pseudo steady state will take place is:

$$t_D = \frac{25}{3}(1 - x_D)^2 \tag{19}$$

The approximation for the second source function and the time limit are:

$$S(y_D, t_D) = \frac{1}{2\sqrt{\pi t_D} L_w}\sqrt{\frac{\eta_x}{\eta_y}} \tag{20}$$

$$t_D = 25 y_D^2 \tag{21}$$

while the approximation and the time limit for the third function are:

$$S(z_D, t_D) = \frac{1}{h} \tag{22}$$

$$t_D = \frac{5}{\pi^2 L_D^2} \tag{23}$$

Therefore the long time approximation of Eq. (1) can be written as follows:

$$P_D(x_D, y_D, z_D, z_{wD}, L_D, t_D) = \frac{q}{2L_w \phi \mu} \int_0^{t_{D1}} S(x_D, \tau_D) \times S(y_D, \tau_D) \times S(z_D, \tau_D) d\tau_D + \frac{1}{2}\int_{t_{D1}}^{t_D} \frac{1}{\tau_D} d\tau_D$$

$$= P_D(x_D, y_D, z_D, z_{wD}, L_D, t_{D1}) + \frac{1}{2}\ln(\frac{t_D}{t_{D1}}) \tag{24}$$

where:

$$t_{D1} \ge Max\begin{bmatrix} \frac{25}{3}(1 - x_D)^2 \\ 25 y_D^2 \\ \frac{5}{\pi^2 L_D^2} \end{bmatrix} \tag{25}$$

In this study, the horizontal wells are classified as short horizontal wells in which $L_D<20$ and long horizontal wells for $L_D>20$ (Long horizontal wells, $L_D>50$ Spivak 1988) (Long horizontal wells, $L_D>10$ Joshi 1991). For long horizontal wells pressure behavior becomes exactly the same behavior as vertical fracture. This fact is related to the function of the infinite plane source in an infinite slab reservoir which is converging to:

$$S(z_D,t_D) = \left[1 + 2\sum_{n=1}^{\infty} \exp\left(-n^2\pi^2 L_D^2 \tau_D\right)\cos(n\pi z_{wD})\cos\left(n\pi(\bar{z}_D + z_{wD})\right)\right] \times \frac{1}{h} = \frac{1}{h} \qquad (26)$$

Therefore the model for long horizontal wells can be written as follows:

$$P_D(x_D,y_D,z_D,z_{wD},L_D,t_D) = \frac{\sqrt{\pi}}{4}\int_0^{t_D} \frac{e^{-\frac{y_D^2}{4t_D}}}{\sqrt{\tau_D}}\left[erf(\frac{1+x_D}{2\sqrt{\tau_D}}) + erf(\frac{1-x_D}{2\sqrt{\tau_D}})\right]d\tau_D \qquad (27)$$

The short time approximation and the applicable time limit are:

$$P_D(x_D,y_D,z_D,z_{wD},L_D,t_D) = \sqrt{\pi t_D}\, e^{-\frac{y_D^2}{4t_D}} - \frac{\pi y_D}{2}erfc\left(\frac{y_D}{2\sqrt{t_D}}\right) \qquad (28)$$

$$t_D = \frac{(1-x_D)^2}{20} \qquad (29)$$

and for wellbore pressure:

$$P_{wD} = \sqrt{\pi t_D} \qquad (30)$$

while the long time approximation and the time limit are the same as regular horizontal well presented in Eq. (24) and Eq. (25).

The pressure response of horizontal wells normally shows three flow regimes: the early radial flow, linear flow, and pseudo-radial flow as shown in **Fig. (2)**. Long horizontal wells may develop two flow regimes only: the linear flow and the pseudo-radial flow as shown in **Fig. (3)**.
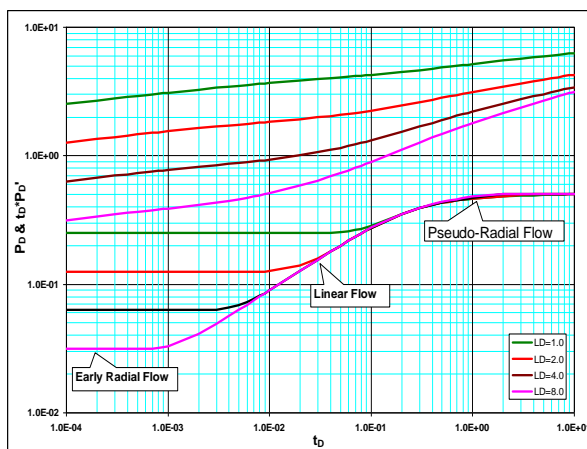
Figure 2: Pressure & pressure derivative long horizontal plot for horizontal wells (LD>20).
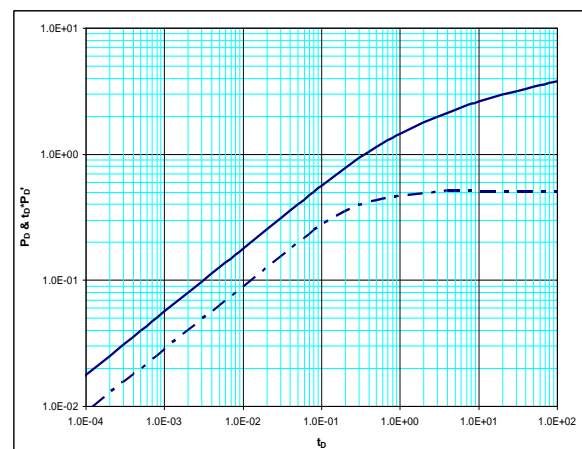
Figure 3: Pressure & pressure derivative plot for wells (LD<20).

Horizontal well in finite reservoir:

The mathematical model that can be used to simulate the pressure behavior created by the constant production of a horizontal well acting on finite or limited reservoir (impermeable boundary), as shown in **Fig. (4)**, also consists of the three instantaneous source solutions (Gringarten and Ramey 1973, Daviau 1988):

$$S(x,t) = \frac{L_w}{x_e}\left[1 + \frac{4x_e}{\pi L_w}\sum_{n=1}^{\infty}\frac{1}{n}\exp(-\frac{\pi^2 n^2 \eta_x^2 t}{4x_e^2})\sin(n\pi\frac{L_w}{2x_e})\cos(n\pi\frac{x_w}{2x_e})\cos(n\pi\frac{x}{2x_e})\right] \tag{31}$$

$$S(y,t) = \frac{1}{2y_e}\left[1 + 2\sum_{n=1}^{\infty}\exp(-\frac{\pi^2 n^2 \eta_y^2 t}{4y_e^2})\cos(n\pi\frac{y_w}{2y_e})\cos(n\pi\frac{y}{2y_e})\right] \tag{32}$$

$$S(z,t) = \frac{1}{h}\left[1 + 2\sum_{n=1}^{\infty}\exp(-\frac{\pi^2 n^2 \eta_z^2 t}{h^2})\cos(n\pi\frac{z_w}{h})\cos(n\pi\frac{z}{h})\right] \tag{33}$$

The pressure behavior model is developed by gathering the above source solutions together:

$$P_D(x_D, y_D, z_D, L_D, x_{eD}, y_{eD}, t_D) =$$

$$\frac{\pi}{2}x_{eD}y_{eD}\int_0^{t_D}\left\{\left[1 + \frac{4}{\pi x_{eD}}\sum_{n=1}^{\infty}\frac{1}{n}\exp(-\frac{\pi^2 n^2 x_{eD}^2 \tau_D}{4})\sin(n\pi\frac{x_{eD}}{2})\cos(n\pi\frac{x_{wD}}{2})\cos(\frac{n\pi}{2}(x_D x_{eD} + x_{wD}))\right]\times\right.$$

$$\left[1 + 2\sum_{n=1}^{\infty}\exp(-\frac{\pi^2 n^2 y_{eD}^2 \tau_D}{4})\cos(n\frac{y_{wD}}{2})\cos(\frac{n\pi}{2}(y_D y_{eD} + y_{wD}))\right]\times \tag{34}$$

$$\left.\left[1 + 2\sum_{n=1}^{\infty}\exp(-n^2\pi^2 L_D^2 \tau_D)\cos(n\pi z_{wD})\cos(n\pi(z_D L_D + z_{wD}))\right]d\tau_D\right.$$

where:

$$x_{wD} = \frac{x_w}{x_e} \tag{35}$$

$$y_{wD} = \frac{y_w}{y_e} \tag{36}$$

$$z_{wD} = \frac{z_w}{h} \tag{37}$$

$$x_{eD} = \frac{L_w}{x_e} \tag{38}$$

$$y_{eD} = \frac{L_w}{y_e}\sqrt{\frac{k_y}{k_x}} \tag{39}$$
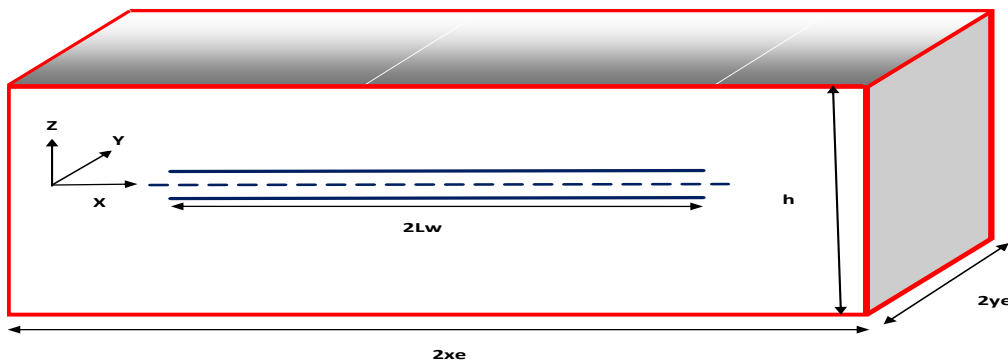
Figure 4: Horizontal well acting in finite reservoir.

Short-time approximation

Short-time approximation can be obtained using the same procedures that have been used for the horizontal well in infinite reservoirs. The first instantaneous function S(x, t) =1 when the monitoring point is located inside the well as the time approaches zero.

$$S(x_D, t_D) = \frac{1}{2\sqrt{\pi \eta_x t}} e^{-\frac{(x-x_w)^2}{4\eta_x t}} = 1 \tag{40}$$

and the proper time limit for the above equation to be applied as determined by Gringarten and Ramey (1973) is:

$$t_D = \frac{(1-x_D)^2}{20} \tag{41}$$

The second instantaneous function S(z, t) has the following formula:

$$S(z_D, t_D) = \frac{1}{2\sqrt{\pi \eta_z t}} e^{-\frac{(z-z_w)^2}{4\eta_x t}} = \frac{1}{2\sqrt{\pi t_D} L_w} \sqrt{\frac{k_x}{k_z}} e^{-\frac{z_D^2}{4t_D}} \tag{42}$$

Since this function deals with the infinite plane source in an infinite slab reservoir, there is a time at which the upper or lower boundary starts to affect the pressure behavior. This time can be estimated by:

$$t_D \leq \min \begin{bmatrix} \dfrac{\left[(\bar{z}_D + 2z_{wD})/L_D \right]^2}{20} \\ \dfrac{\left[(\bar{z}_D + 2z_{wD} - 2)/L_D \right]^2}{20} \end{bmatrix} \tag{43}$$

while the third instantaneous function S(y, t) has the following formula for the short time approximation:

$$S(y_D, t_D) = \frac{1}{2\sqrt{\pi \eta_y t}} e^{-\frac{(y-y_w)}{4\eta_y t}} = \frac{1}{2\sqrt{\pi t_D} L_w} \sqrt{\frac{\eta_x}{\eta_y}} e^{-\frac{y_D^2}{4t_D}} \tag{44}$$

and the proper time for this approximation to be applicable is:

$$t_D \leq \min \begin{bmatrix} \dfrac{\left[(y_D y_{eD} + 2y_{wD})/y_{eD} \right]^2}{20} \\ \dfrac{\left[(y_D y_{eD} + 2y_{wD} - 4)/y_{eD} \right]^2}{20} \end{bmatrix} \tag{45}$$

Based on the short time approximations for the above three functions, the short time approximation for Eq. (34) can be written as the product of the three approximations:

$$P_D(x_D, y_D, z_D, z_{wD}, L_D, t_D) = \frac{1}{4L_D} \int_0^{t_D} \frac{1}{\tau_D} e^{-\frac{[y_D^2 + z_D^2]}{4\tau_D}} d\tau_D = -\frac{1}{4L_D} Ei\left(-\frac{y_D^2 + z_D^2}{4t_D} \right)$$

$$= \frac{1}{4L_D} \left(\ln\left(\frac{t_D}{y_D^2 + z_D^2} \right) + 0.80907 \right) when \ Ei\left(-\frac{y_D^2 + z_D^2}{4t_D} \right) \leq 0.01 \tag{46}$$

Long-time approximation
As the time increases, the exponential terms in Eq. (31), (32), and (33) approach zero. Therefore, the first instantaneous function can be approximated as follows:

$$S(x, t) = \frac{L_w}{x_e} \tag{47}$$

and the long limit of the time so that the pseudo steady state will take place is:

$$t_D \geq \frac{20}{\pi^2 x_{eD}^2} \tag{48}$$

The approximation for the second source function and the time limit are:

$$S(y, t) = \frac{1}{2y_e} \tag{49}$$

$$t_D \geq \frac{20}{\pi^2 y_{eD}^2} \tag{50}$$

while the approximation and the time limit for the third function are:

$$S(z,t) = \frac{1}{h} \tag{51}$$

$$t_D \geq \frac{5}{\pi^2 L_D^2} \tag{52}$$

Therefore the long time approximation of Eq. (34) can be written as follow:

$$P_D(x_D, y_D, z_D, z_{wD}, L_D, t_D) = \frac{q}{2L_w \phi \mu} \int_0^{t_{D1}} S(x_D, \tau_D) \times S(y_D, \tau_D) \times S(z_D, \tau_D) d\tau_D + \frac{q}{2\phi \mu L_w} \int_{t_{D1}}^{t_D} \frac{Lw}{x_e y_e h} d\tau_D \tag{53}$$

$$= P_D(x_D, y_D, z_D, z_{wD}, L_D, t_{D1}) + \frac{\pi}{2} x_{eD} y_{eD} (t_D - t_{D1})$$

where:

$$t_{D1} \geq Max \begin{bmatrix} \dfrac{20}{\pi^2 x_{eD}^2} \\[2ex] \dfrac{20}{\pi^2 y_{eD}^2} \\[2ex] \dfrac{5}{\pi^2 L_D^2} \end{bmatrix} \tag{54}$$

For long horizontal wells when $L_D \geq 20$, where the vertical fracture pressure behavior is expected to happen, the infinite plane source in slab reservoir can be presented as:

$$S(z_D, t_D) = \left[1 + 2\sum_{n=1}^{\infty} \exp\left(-n^2 \pi^2 L_D^2 \tau_D\right) \cos(n\pi z_{wD}) \cos\left(n\pi(\bar{z}_D + z_{wD})\right) \right] \times \frac{1}{h} = \frac{1}{h} \tag{55}$$

Therefore the model for long horizontal wells in limited reservoirs can be written as follows:

$$P_D(x_D, y_D, z_D, L_D, x_{eD}, y_{eD}, t_D) =$$

$$\frac{\pi}{2} x_{eD} y_{eD} \int_0^{t_D} \left\{ \left[1 + \frac{4}{\pi x_{eD}} \sum_{n=1}^{\infty} \frac{1}{n} \exp(-\frac{\pi^2 n^2 x_{eD}^2 \tau_D}{4}) \sin(n\pi \frac{x_{eD}}{2}) \cos(n\pi \frac{x_{wD}}{2}) \cos(\frac{n\pi}{2}(x_D x_{eD} + x_{wD})) \right] \times \right. \tag{56}$$

$$\left. \left[1 + 2\sum_{n=1}^{\infty} \exp(-\frac{\pi^2 n^2 y_{eD}^2 \tau_D}{4}) \cos(n\frac{y_{wD}}{2}) \cos(\frac{n\pi}{2}(y_D y_{eD} + y_{wD})) \right] d\tau_D \right.$$

The short time approximation and the applicable time limit for long horizontal wells in limited reservoirs are the same for long horizontal wells in infinite reservoirs. The long time approximation and the time limit are the same as the regular horizontal wells in limited reservoirs.

Pressure behavior

In general, the pressure response of horizontal wells acting in finite reservoirs shows five flow regimes: the early radial flow, early linear flow, pseudo- radial flow, channel flow (linear flow corresponding to the channel system when the pressure behavior is affected by the influence of the nearest parallel boundaries to the horizontal wells), and pseudo-steady state flow. The following classification for the pressure behavior can be noticed based on the distance to the boundaries.

1- Square reservoir:

The effect of the boundaries depends significantly on the distance to the nearest boundary which is normal to the direction of the wellbore in the case of square reservoirs. Four flow regimes are expected to develop: early radial, early linear, pseudo-radial and pseudo steady state for $x_{eD} = y_{eD} \leq 0.5$ as shown in **Fig. (5)** and **Fig. (6)**. For $x_{eD} = y_{eD} \geq 0.5$, pseudo-radial flow are disappeared and linear flow or channel flow for

$x_{eD} = y_{eD} = 1.0$ will be the dominant flow between the early radial and pseudo-steady state flow as shown in Fig. **(7)** and Fig. **(8)**. For large square drainage area $x_{eD} = y_{eD} = 0.1$, pseudo-steady state flow is affected by wellbore length. The required time to reach pseudo-steady state increases as the wellbore length increases as shown in Fig.(5). However, when both x_{eD} and y_{eD} increase, the required time to reach pseudo-steady state becomes constant for all wellbore length as shown in Figs. (6), (7) and (8).
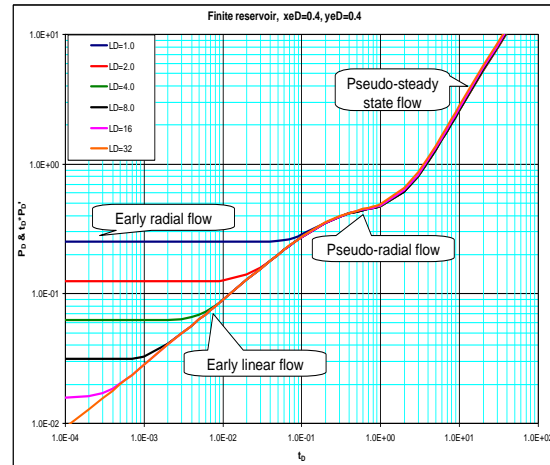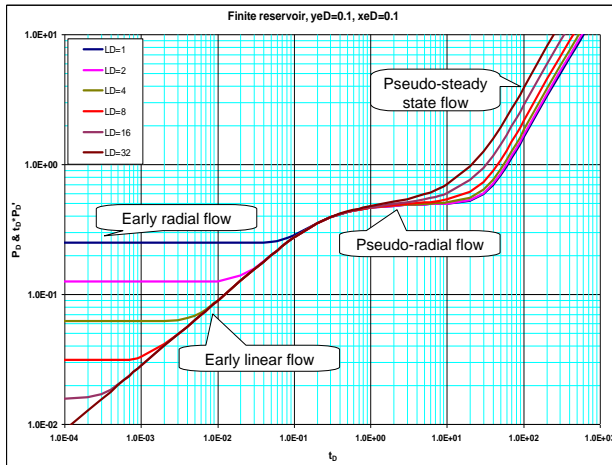
Figure 5: Pressure derivatives for different horizontal wells. Figure 6: Pressure derivatives for different horizontal wells.
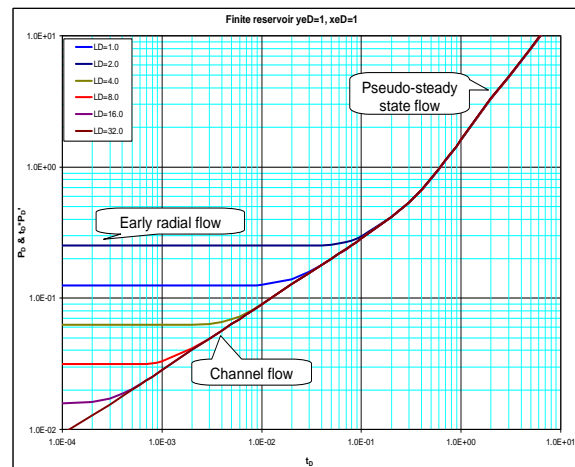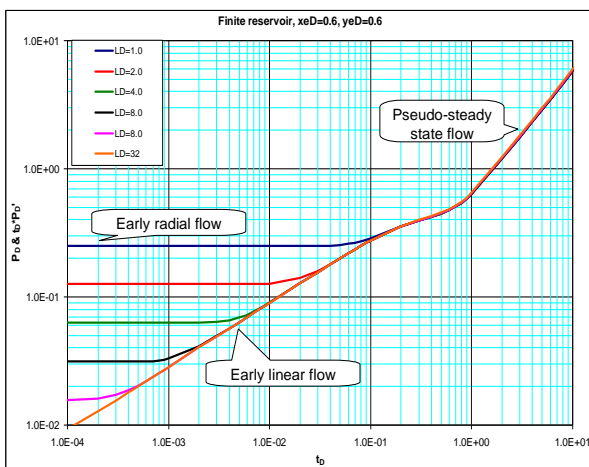
Figure 7: Pressure derivatives for different horizontal wells. Figure 8: Pressure derivatives for different horizontal wells

2- Rectangular reservoirs $0.1 < xeD < 0.5 \ and \ 0.1 < yeD < 0.5$

Typically, early linear, pseudo-radial and pseudo-steady state flow are observed in addition to early radial flow for the case of $L_D \le 20$. The required time to reach pseudo-steady state is affected by the distance to the boundaries. It increases as the distance increases regardless of the wellbore length as shown in **Fig. (9)** and **(10)**.
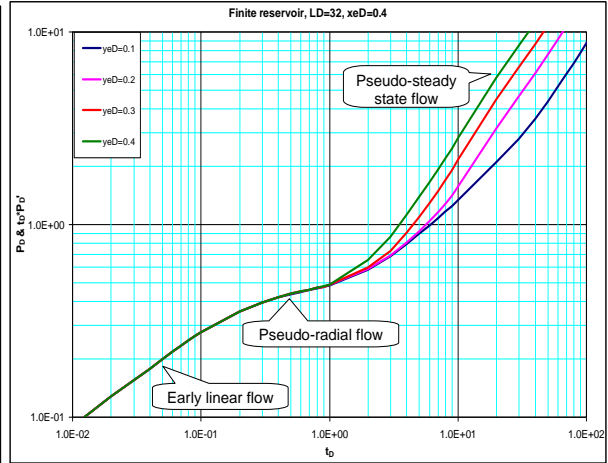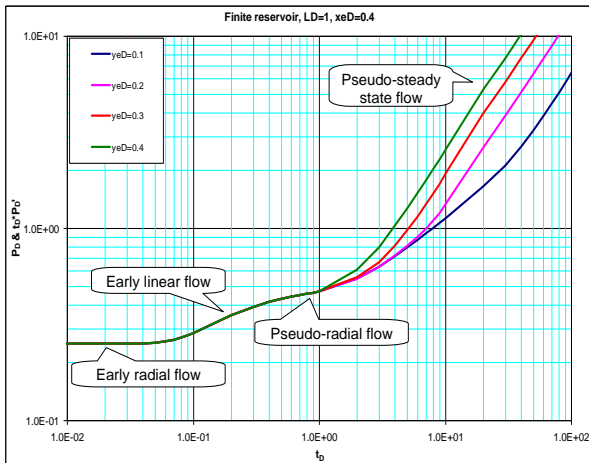
Figure 9: Pressure derivatives for different horizontal wells. Figure 10: Pressure derivatives for different horizontal wells.

3- Rectangular reservoirs $1 \le xeD < 0.5 \ and \ 1 \le yeD < 0.5$

Two flow regimes are observed for horizontal well with $L_D \ge 20$, channel and pseudo-steady state flow as shown in **Fig. (12)**. Early radial flow is observed for wellbore $L_D \le 20$ as shown in **Fig. (11)** in addition to the channel and pseudo-steady state flow.
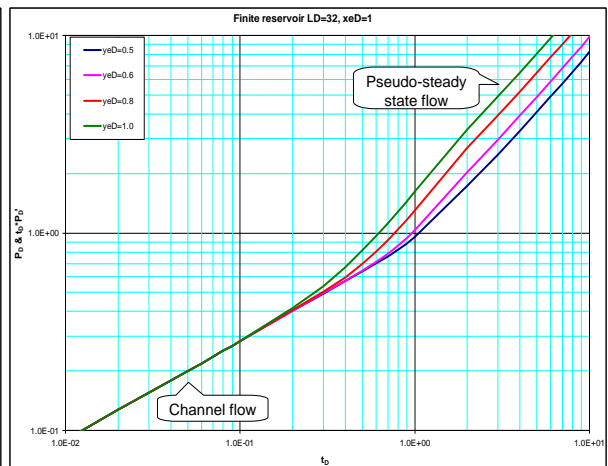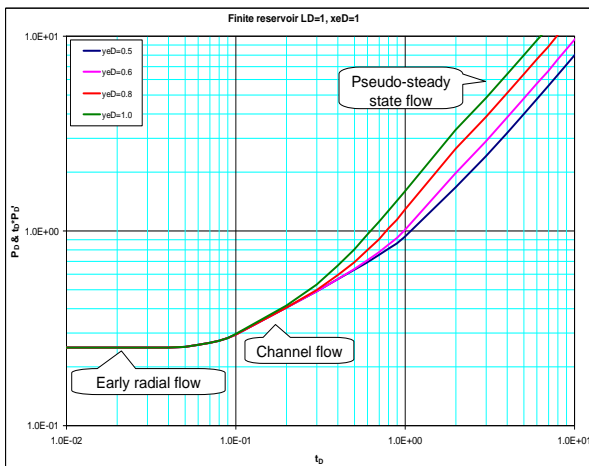
Figure 11: Pressure derivatives for different horizontal wells. Figure 12: Pressure derivatives for different horizontal wells.

Flow Regimes:
1- Early radial flow:

For horizontal wells with $L_D \le 20$, early vertical radial flow is expected to develop at early time as the fluid flows radially from all directions in YZ plane into the wellbore as shown in **Fig. (13)**. This flow regime is characterized by slope equals to $\left(1/4L_D\right)$ on pressure curves or having the following value on pressure derivative curves:

$$(t_D \times P_D')_{ER} = \frac{0.5}{2L_D} \tag{57}$$

therefore:

$$(t \times \Delta P')_{ER} = \frac{70.6q\mu B}{\sqrt{k_z k_y}L} \tag{58}$$

or:

$$(\Delta P)_{ER} = \frac{162.6q\mu B}{\sqrt{k_z k_y}\, L}\log(t) + C \tag{59}$$

where:

$$C = \ln(\frac{k_y}{\phi\mu cr_w^2}) - 7.43 + 2S_d \tag{60}$$

$$S_d = S\left(\frac{L}{h}\sqrt{\frac{k_z}{k_y}}\right) \tag{61}$$

Therefore, a semi-log plot of (ΔP) vs. (t) yields a straight line during the early data. The slope of this line can be used to calculate:

$$\sqrt{k_z k_y} = \frac{162.56q\mu B}{m_{ER} L} \tag{62}$$

2- Early linear flow:

After both upper and lower boundaries are reached, early linear flow is developed. Early linear flow represents linear flowing of reservoir fluids in the XZ plane toward the wellbore as shown in **Fig.(14)**. This flow is characterized by half slope on pressure derivative curves. The governing equation for early linear flow (Goode 1987) is:

$$(\Delta P)_{EL} = \frac{8.128qB}{Lh}\sqrt{\frac{\mu t}{k_y \phi c_t}} + C \tag{63}$$

Where:

$$C = \frac{141.2q\mu B}{L\sqrt{k_z k_y}}S_d \tag{64}$$

$$S_d = \frac{L\sqrt{k_z k_y}}{141.2q\mu b}\bigg|_{\Delta P=0} - \ln\left(\frac{h}{r_w}\right) - 0.25\ln\left(\frac{k_y}{k_z}\right) + 1.838 \tag{65}$$

Eq. (74) indicates that the plot of ΔP vs. $t^{1/2}$ yields a straight line. The slope of this line m_{EL} can be used to estimate k_y.

$$\sqrt{k_y} = \frac{8.128qB}{Lhm_{EL}}\sqrt{\frac{\mu}{\phi c}} \tag{66}$$
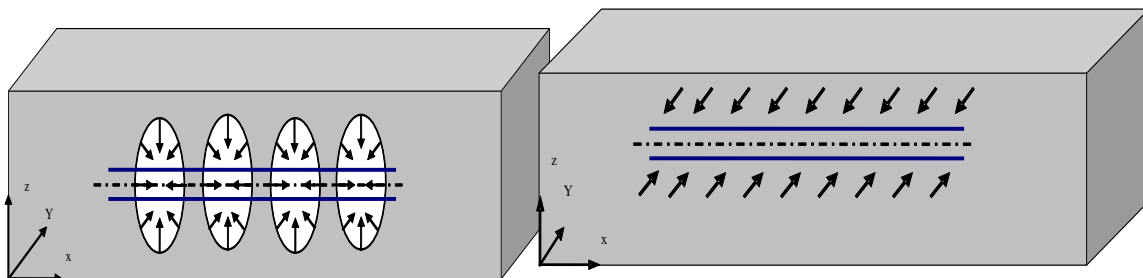
Figure 13: Early radial flow.　　　　　Figure 14: Early linear flow.

3- Pseudo radial flow:

Late or pseudo-radial flow takes place when the dimensionless time reaches the limits defined by Eq. (25) for horizontal well acting on an infinite reservoir or Eq. (54) for a finite reservoir. This flow represents

radial flowing of reservoir fluid in the XY plane toward the wellbore as shown in **Fig. (15)**. For short distance to the boundary $1 \leq xeD < 0.5$ *and* $1 \leq yeD < 0.5$, pseudo-radial flow can not be observed. This type of flow is characterized by horizontal line on pressure derivative curve with:

$$(t_D \times P_D')_{PR} = 0.5 \tag{67}$$

$$(t \times \Delta P')_{PR} = \frac{70.6q\mu B}{\sqrt{k_x k_y} h} \tag{68}$$

$$(\Delta P)_{PR} = \frac{162.6q\mu B}{\sqrt{k_x k_y} h} \log(t) + C \tag{69}$$

$$C = \frac{162.6q\mu B}{\sqrt{k_x k_y} h}[\log\left(\frac{k_x}{\phi\mu c L^2}\right) - 2.023] + \frac{141.2q\mu B}{L\sqrt{k_y k_z}} S_d \tag{70}$$

$$S_d = 1.151\sqrt{\frac{k_z}{k_x}} \frac{L}{h}\left[\frac{\Delta P_{1hr}}{m_{PR}} - \log(\frac{k_x}{\phi\mu c L^2}) + 1.76\right] \tag{71}$$

A semi-log plot of (ΔP) vs. (t) yields a straight line during the pseudo-radial flow period. The slope of this line can be used to calculate:

$$\sqrt{k_x k_y} = \frac{162.6q\mu B}{m_{PR} h} \tag{72}$$
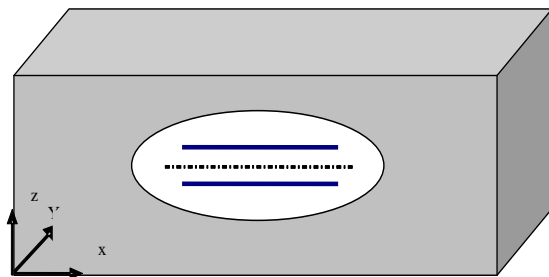
Figure 15: Pseudo-radial flow.   **Figure 16: Cahnnel flow.**
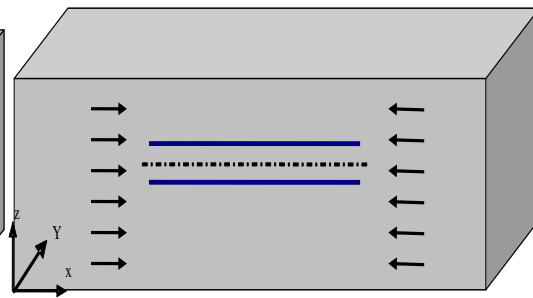
4 - Channel Flow:

       This flow starts when the pressure behavior is affected by the closest parallel outer boundaries of the reservoir. It takes place either in the XZ plane or YZ plane as shown in Fig.(16). It is characterized by slope of half on pressure derivative curves. The governing equation for this flow is (Goode 1987):

$$(\Delta P)_{CF} = \frac{8.128qB}{2hx_e}\sqrt{\frac{\mu t}{k_y \phi c_t}} + C \tag{73}$$

$$C = \frac{141.2q\mu B}{L\sqrt{k_z k_y}} S_t \tag{74}$$

$$S_t = \frac{L}{2x_e}\left[\left.\frac{2x_e\sqrt{k_z k_y}}{141.2q\mu b}\right|_{\Delta P=0} - S_p - \ln(\frac{h}{r_w}) - 0.25\ln(\frac{k_y}{k_z}) + 1.838\right] \tag{75}$$

where S_p represents the partial penetration skin factor.

The plot of ΔP vs. $t^{1/2}$ yields a straight line. The slope of this line m_{CF} can be used to estimate x_e.

$$x_e = \frac{8.128qB}{2hm_{CF}}\sqrt{\frac{\mu}{k_y \phi c_t}} \tag{76}$$

5- Pseudo-Steady State Flow:

For long producing time in a closed reservoir, a pseudo-steady state flow regime appears as a result of the pressure being influenced by all four closed boundaries at the same time. It is characterized by unit-slop line on the pressure derivative curve. The equation of this straight line is:

$$\left(t_D \times P_D{'}\right)_{pss} = 2\pi t_{DA} \tag{77}$$

This flow can be used to estimate the drainage area of the reservoir:

$$A = \frac{0.2338qB}{\phi c_t h}\sqrt{\frac{k_x}{k_y}}\left(\frac{t_{PSS}}{\left(t \times \Delta P{'}\right)_{PSS}}\right) \tag{78}$$

Application of Type Curve Matching:

As shown on the plots in Appendix (A), the pressure and pressure derivative have a unique shape for each combination of the distance to the outer boundaries x_e and y_e (reservoir configuration). These plots can be used for the type-curve matching technique to determine reservoir characteristics such as: permeability in the three directions and the distance to the boundaries. The following steps illustrate the procedures required in this technique:

1- Plot (ΔP vs. t) and ($t \times \Delta P{'}$ vs. t) on log-log paper.
2- Obtain the best match of the data with one of the type curves.
3- Read from any match point: $t_M, \Delta P_M, t_{DM}, P_{DM}, L_D, x_{eDM}, y_{eDM}$.

4- Calculate k_x, k_y, k_z from the following equations:

$$k_x = \frac{\phi \mu c_t L_w^2 t_{DM}}{0.0002637 t_M} \tag{79}$$

$$k_y = \frac{1}{k_x}\left[\frac{141.2q\mu B P_{DM}}{h\Delta P_M}\right]^2 \tag{80}$$

$$k_z = \left(\frac{L_D^2 h^2}{L_w^{\,2}}\right)k_x \tag{81}$$

5-   Calculate x_e using:

$$x_e = \frac{L_w}{x_{eDM}} \tag{82}$$

6-   Calculate y_e using:

$$y_e = \frac{L_w}{y_{eDM}}\sqrt{\frac{k_y}{k_x}} \tag{83}$$

II.   EXAMPLE

A pressure drawdown test data of a horizontal well acting on a finite reservoir are given in Table B-1 of Appendix (B). Other known reservoir and well data are:

q = 500 STB/D ϕ = 0.1 μ = 0.5 cp
c_t = 2x10^{-6} psi^{-1} B = 1.15 bbl/STB   h = 50 ft
 L=1600 ft r_w = 0.63 ft p_i = 9500 psi
Estimate formation permeability in all direction and the distance to the outer boundaries.

III.   SOLUTION

1-The pressure and pressure derivative plot is shown in **Fig. (17)**.
2- The matching process is shown in **Fig. (18)**.
3- Read from the matching point:

$$t_M = 10, t_{DM} = 0.33, \Delta P_M = 10, P_{DM} = 0.078, L_{DM} = 8, x_{eDM} = 0.4, y_{eDM} = 0.3$$

4- The permeabilities in the x, y, z directions from Eqs. (79, 80, 81):

$$k_x = \frac{0.1 \times 0.5 \times 0.00002 \times 800^2 \times 0.33}{0.0002637 \times 10} = 8 \; md$$

$$k_y = \left[\frac{141.2 \times 500 \times 0.5 \times 1.15 \times 0.078}{\sqrt{8} \times 50 \times 10} \right]^2 = 5 \; md$$

$$k_H = \sqrt{k_x k_y} = \sqrt{8 \times 5} = 6.3 \; md$$

$$k_z = k_V = \frac{8^2 \times 50^2 \times 8}{800^2} = 2 \; md$$
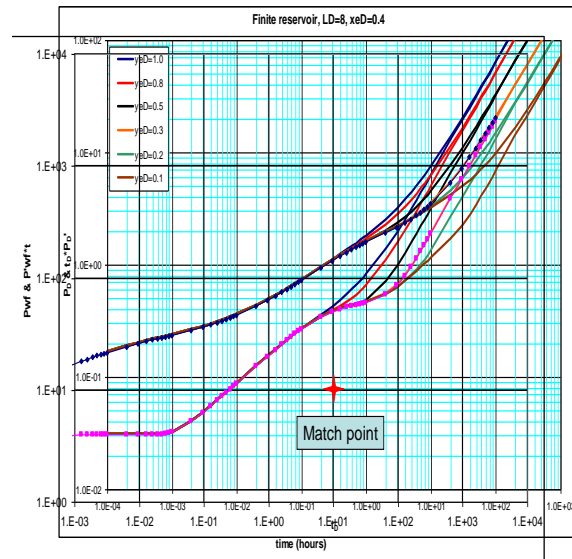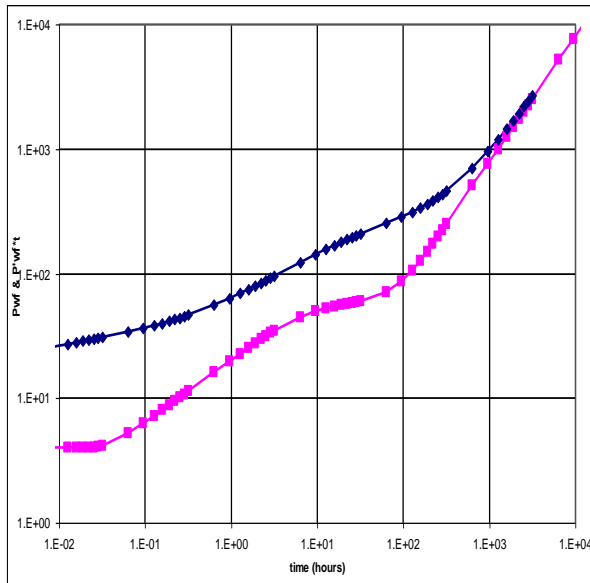
Fig. (17): Pressure & pressure derivative plots for Example.   Fig. (18): Type curve matching.

5-The distance to the boundary in the x-direction using Eq. (82):

$$x_e = \frac{800}{0.4} = 2000 \; ft$$

6-The distance to the boundary in the y-direction using Eq. (83):

$$y_e = \frac{800}{0.3} \sqrt{\frac{5}{8}} = 2108 \; ft$$

The above results can be compared with the results obtained by the conventional semilog method as follow:

1- The Cartesian plot of ΔP vs. $\sqrt{t}$, as shown in **Fig. (19)**, yields a straight line corresponding to the early linear flow data. This slope of this line $m_{EL} = 41$ can be used to obtain k_y using Eq. (66):

$$k_y = \left[\frac{8.128 \times 500 \times 1.15}{1600 \times 41 \times 50} \right]^2 \frac{0.5}{0.1 \times 0.000002} = 5 \; md$$

2 - From early time data, the semi-log plot of the early radial flow, as shown in **Fig. (20)**, can be used to obtain k_z from the slope of the straight line $m_{ER} = 9.3$ using Eq. (62).

$$k_z = \left[\frac{162.6 \times 0.5 \times 500 \times 1.15}{9.3 \times 1600 \times \sqrt{5}} \right]^2 = 2 \ md$$

3- From late time data, the semi-log plot of the pseudo-radial flow as shown in **Fig. (21)** can be used to obtain k_x from the slope of the straight line $m_{PR} = 147$ using Eq. (72).

$$k_x = \left[\frac{162.6 \times 500 \times 0.5 \times 1.15}{147 \times 50 \times \sqrt{5}} \right]^2 = 8 \ md$$
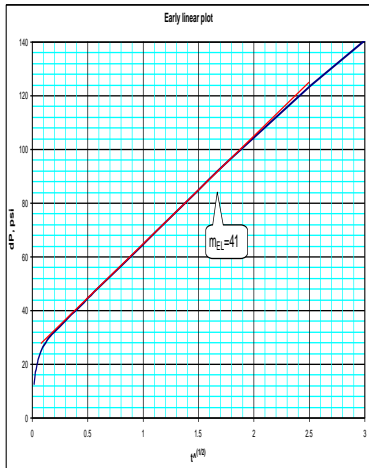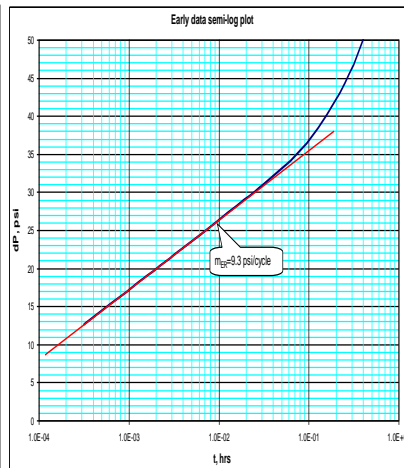
Early linear plot	Early data semi-log plot	Pseudo-radial semi-log plot
$m_{EL}=41$	$m_{BR}=9.3$ psi/cycle	$m_{PR}=147$
Fig. (19): Early-Linear plot	Fig. (20): Early-radial plot.	Fig. (21): Pseudo-Radial plot.
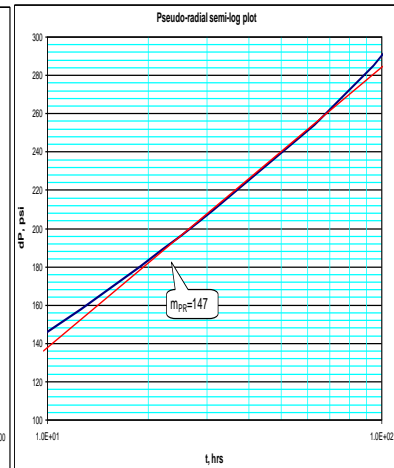
IV.   CONCLUSIONS

1-Pressure behavior and flow regimes of horizontal wells acting in bounded reservoirs are affected significantly by the outer boundaries where the reservoir no longer maintains constant pressure when the production pulse reaches theses boundaries.

2-The impact of the boundaries on pressure responses and fluid flow regimes occur at late time production. Pressure behaviors and flow regimes at early time production are not affected by the boundaries.

3-Wellbore length has noticeable effect on pressure behavior at late time for large square drainage area. However, this effect has not been observed for rectangular shape reservoirs.

4- Pseudo-steady state flow represents the flow resulted due to the impact of the boundaries. The starting time of this type of flow depends mainly on the distance to the boundaries and somehow a wellbore length. For the same wellbore length, it increases as the distance to the boundary increases.

5- Channel flow usually occurs for the following cases:
- The distance to one of the boundaries is significantly smaller than the second boundary.
- The wellbore penetrates completely the formation in the long horizontal direction.
- Square drainage area where the boundary in the normal plane to the wellbore can be reached before the other boundary which is parallel to the wellbore.

6-The pressure behavior of the long horizontal well, i.e. $L_D > 20$, is similar to the behavior of vertical fractures. Early radial flow can't be seen for long horizontal wells.

7- Permeabilities in all three directions and well location with respect to the boundaries can be estimated using type curve matching technique.

Nomenclature
A   drainage area, ft^2
B   oil volumetric factor, RB/STB
c_t compressibility, 1/psi
h   formation thickness, ft
k_x Formation permeability in the X direction, md
k_y Formation permeability in the Y direction, md
k_z Formation permeability in the Z direction, md
L   total length of horizontal well, ft
L_w half length of horizontal well, ft

m_{ER} slope of early radial flow line
m_{EL} slope of early linear flow line
m_{PR} slope of pseudo-radial flow line
m_{CF} slope of channel flow line
P   pressure, psi
P_D dimensionless pressure
P_i initial pressure, psi
P_{wf} flowing well pressure, psi
Q   oil well flow rate per unit length of horizontal well, B/D/ft
q   oil well flow rate, B/D
r_w wellbore radius, ft
S   pseudo-skin factor
t   time, hr
t_D dimensionless time
t_p producing time, hr
t_{pss} pseudo-steady state time, hr
x_e half the distance to the boundary in the X direction, ft
x_w the X coordinate of the production point.
y_e half the distance to the boundary in the Y direction, ft
y_w the Y coordinate of the production point.
z_w the Z coordinate of the production point.

GREEK SYMBOLS

ϕ Porosity
μ viscosity, cp
⬜⬜⬜⬜⬜⬜⬜⬜⬜⬜ dummy variable of time

SUBSCRIPTS

CF   channel flow
ER   early radial flow
EL   early linear flow
PR   pseudo radial flow
PSS   pseudo-steady state flow

V.   REFERENCES

[1].   Babu, D.K., and Odeh, A.S. 1988. Productivity of a Horizontal Well" SPE 18298 presented at the 63rd Annual Technical Conference, Houston, 2-5 October.doi: 102118/18334-MS.
[2].   Carvalho, R.S., and Rosa, A.J. 1989. A Mathematical Model for Pressure Evaluation in an infinite-Conductivity Horizontal well. SPE Formation Evaluation 4 (4): 559-566. SPE 15967-PA. doi:102118/15967-PA.
[3].   Clonts, M.D., and Ramey, H.J. 1986. Pressure Transient Analysis for Wells with Horizontal drainholes. SPE 15116 presented at the SPE Regional Meeting, California, 2-4 April. doi: 102118/15116-MS.
[4].   Daviau, F., Mouronval, G., Bourdarot, G., et al. 1988. Pressure Analysis for Horizontal Wells. SPE Formation Evaluation: SPE Formation Evaluation: 717-724. SPE 14251-PA. doi: 102118/14251-PA.
[5].   Escobar, Freddy H., Nestor F. Saavedra, Claudia M. Hernandez, et al. 2004. Pressure and Pressure Derivative Analysis for Linear Homogeneous Reservoirs without using Type-Curve matching. SPE 88874 presented at the 28th annual SPE technical conference and exhibition in Abuja, Nigeria, 2-4 August. doi: 102118/88874-MS.
[6].   Economides, M.J., Brand, C.W., Frick, T.P. 1996.Well Configurations in Anisotropic Reservoirs. SPE Formation Evaluation.257-262. SPE 27980-PA. doi: 102118/27980-PA.
[7].   Giger, F. 1985. Horizontal Wells Production Techniques in Heterogeneous Reservoirs. SPE 13710 presented at the Middle East oil technical conference, Bahrain, 11-14 March. doi: 102118/13710-MS.
[8].   Goode, P.A., and Kuchuk, F.J.: 1991. Inflow Performance of Horizontal Wells. SPE Reservoir Engineering. 319-323. SPE 21460-PA.doi: 102118/21460-PA.
[9].   Goode, P. A. and Thambynaygam, R.K.M. 1987. Pressure Drawdown and buildup Analysis of Horizontal Wells in Anisotropic Media. SPE Formation Evaluation. 683-697. SPE 14250-PA. doi: 102118/14250-PA.
[10]. Gringarten, A. C. 2010. Practical Use of Well Test Deconvolution," SPE 134534 presented at the 2010 annual technical conference, Florence, 20-22 September. Doi: 10218/134534-MS.
[11]. Gringarten, A. C., Ramey, H. J. 1973. The Use of Source and Green's Function in Solving Unsteady-Flow Problem in Reservoir. SPEJ. 285-295. SPE 3818. doi: 102118/3818-PA.
[12]. Gringarten, A.C., Von Schoreter, T., Rolfsavaag, T., et al. 2003. Use of Downhole Pressure Gauge Data to Diagnose Production Problems in a North Sea Horizontal Well. SPE 84470 presented at the 2003 annual conference, Denver, 5-8 October. Doi:102118/84470-MS.
[13]. Guo, G., and Evans, R.D. 1993. An Economic Model for Assessing the Feasibility of exploiting Naturally Fractured Reservoirs by Horizontal Well technology. SPE 26676 presented at the 68th Annual technical Conference, Houston, 3-6 October. doi: 102118/26676 MS
[14]. Hashemi, A., Laurent, M., and Gringarten, A.C. 2004. Well test Analysis of Horizontal Wells in Gas-condensate reservoirs. SPE 89905 presented at the SPE Annual Technical Conference, Houston, 26-29 September. doi: 102188/89905-MS.
[15]. Ilk, D., Valko, P.P., and Blasingame. 2005. Deconvolution of Variable Rate Reservoir Data Using B-Spline. SPE 95571 presented at the 2005 annual conference, Dallas, 9-12 October. doi: 102118/95571-MS.

[16].   Joshi, S.D. 1986. Augmentation of Well Productivity Using Slant and Horizontal Wells. SPE 15375 paper presented at the 61th annual technical conference, New Orleans, 5-8 October. doi: 102188/15375-MS.

[17].   Khelifa, M., and Tiab, D. 2002. Multirate Test in Horizontal Wells. SPE 77951 paper presented at the SPE Asia Pacific Oil and gas conference, Melbourne, 8-10 October. doi: 102188/77951-MS.

[18].   Kuchuk, F.J., Goode, P.A., Wilikinson, D.J., Thambynayagam, R.K. 1991. Pressure-Transient behavior of Horizontal wells with and without gas Cap or aquifer. SPE Formation Evaluation. 86-94. SPE 17413-PA. doi: 102118/17413-PA.

[19].   Odeh, A.S., and Babu, D.K. 1990. Transient Flow Behavior of Horizontal wells: Pressure Drawdown and Buildup analysis. SPE Formation Evaluation. 7-15. SPE 18802-PA. doi: 102118/18802-PA.

[20].   Ogunsanya, B.O., Oetama, T.P., Heinze, J.F., et al. 2005. A Pysically Consistent Model for describing Transient Pressure Behavior of Horizontal drainholes. Canadian SPE 2005-071 presented at the 6th Canadian International Petroleum Conference, Calgary, Alberta, 7-9 June.

[21].   Ozkan, E., Raghavan, R., and Joshi, S.D. 1989. Supplement for SPE 16378, Horizontal Well Pressure analysis. SPE 20271 availble from Richardson, TX 75083-3836.

[22].   Ozkan, E., Sarica, C., Haciislamoglu, M., et al. 1995. Effect of Conductivity on Horizontal Well Pressure behavior. SPE Advanced Technology Series Vol. 3, No.1. 85-94. SPE 24683-PA. doi: 102118/24683-PA.

[23].   Spivak, D. 1985. Pressure Analysis for Horizontal Wells. Ph.D. Dissertation, Louisiana Tech University, Loisiana (May 1985).

[24].   Verga, F.M., Beretta, E., and Albani, D. 2001. Transient Dual-Porosity Behavior for Horizontal wells draining Heterogeneous Reservoirs. SPE 68844 presented at the SPE western Regional Meeting, California, 26-30 March. doi: 102118/68844-MS.

[25].   Thompson, L.G., and Temeng, K.O. 1993. Automatic Type-Curve matching for Horizontal wells. SPE 25507 presented at the production operation symposium, Oklahoma City, 21-23 March. doi: 102118/25507-MS.

[26].   Von Schroeter, T., Hollaender, F., and Gringarten, A.C. 2004. Deconvolution of Well Test Data as a Nonlinear Total Least squares Problem. SPE Journal. 375-390. SPE 77688-PA. doi: 102118/77688-PA.

[27].   Whittle, T., Jiang, H., Young, S., and Gringarten, A.C. 2009. Well Production Forecasting by Extrapolation of the Deconvolution of the Well Test Pressure Transients. SPE 122299 presented at the 2009 SPE EUROPEC/EAGE conference, Netherland, 8-11 June. doi: 102118/122299-MS.

Appendix A
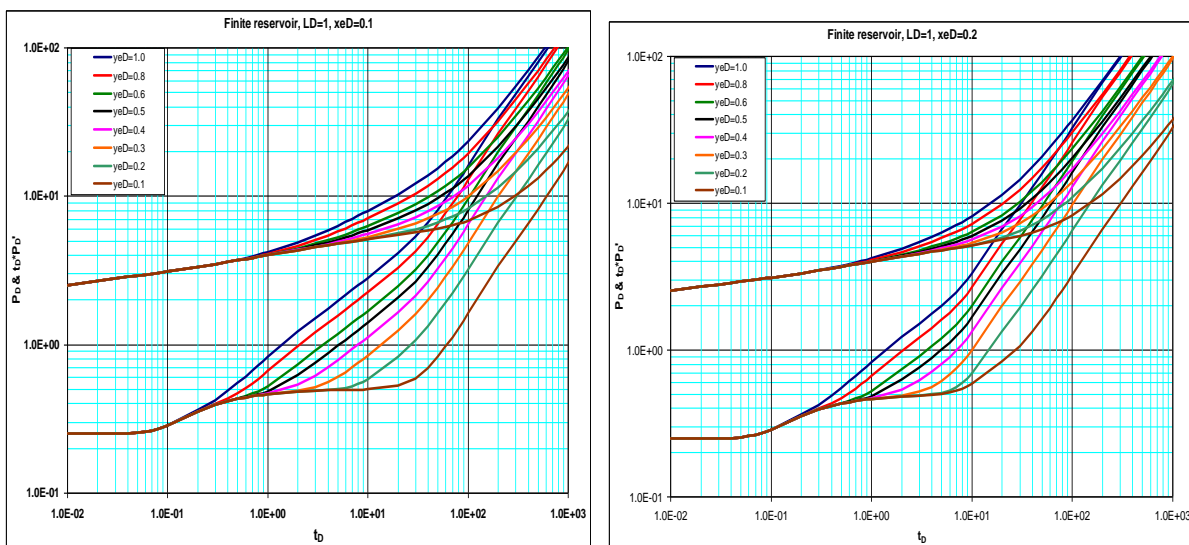
Fig. (A-1): Type curve for short horizontal well L_D=1 Fig. (A-2): Type curve for short horizontal well L_D=1.
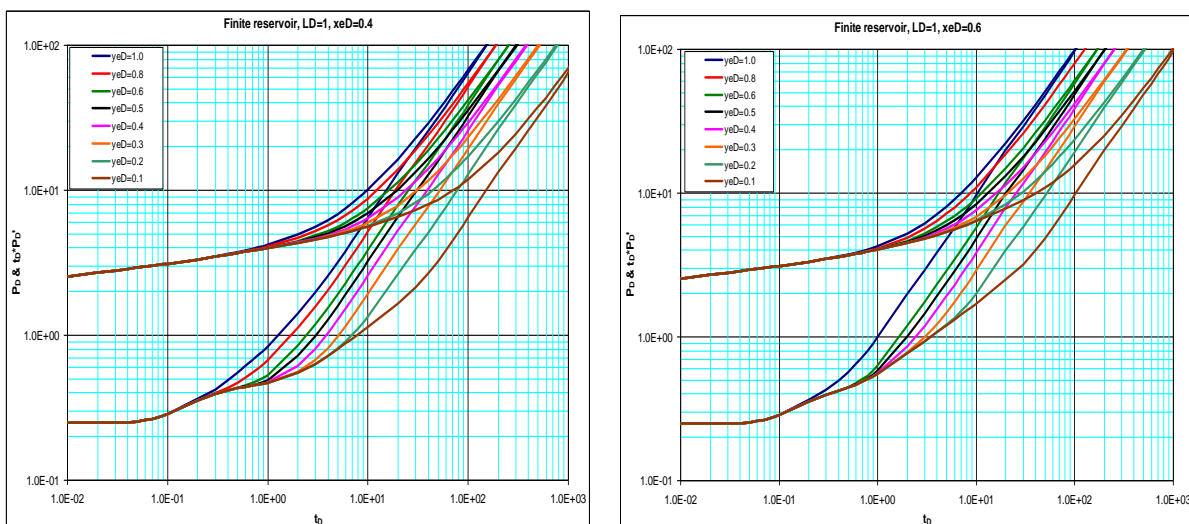
Fig. (A-3): Type curve for short horizontal well $L_D=1$.   Fig. (A-4): Type curve for short horizontal well $L_D=1$.
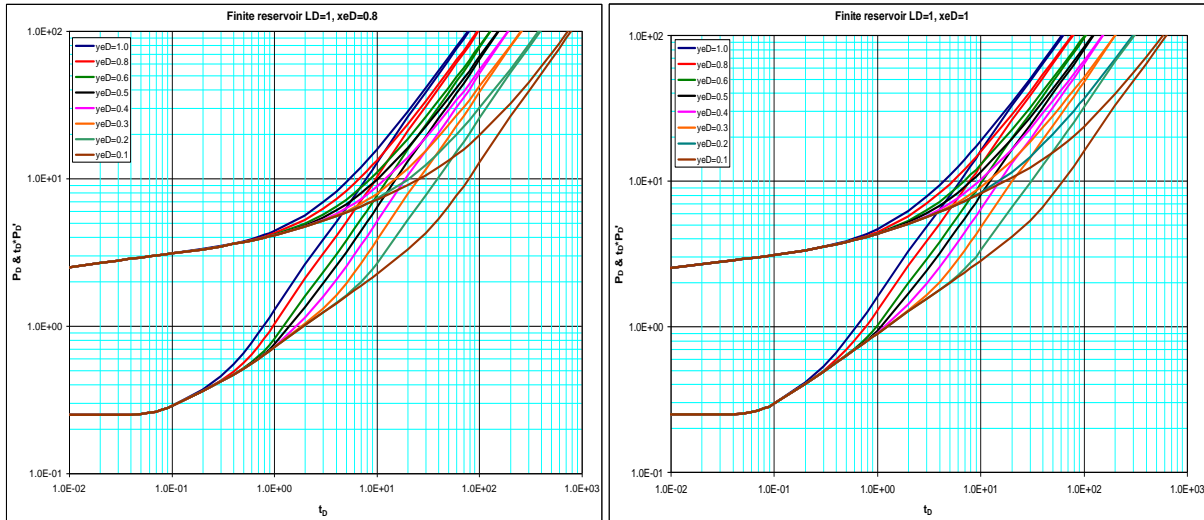
Fig. (A-5): Type curve for short horizontal well $L_D=1$. Fig. (A-6): Type curve for short horizontal well $L_D=1$.
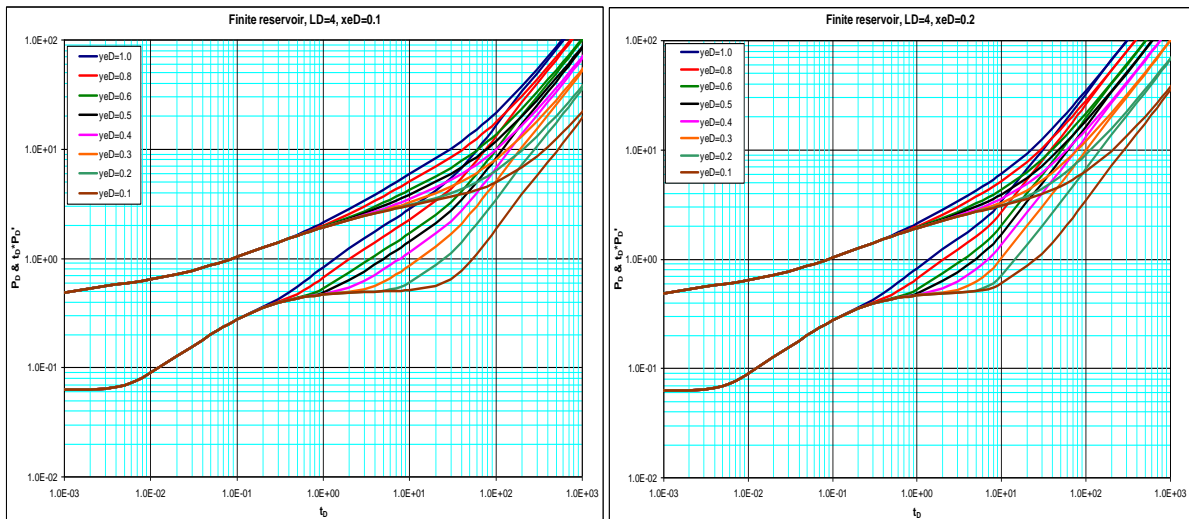
Fig. (A-7): Type curve for short horizontal well $L_D=4$.   Fig. (A-8): Type curve for short horizontal well $L_D=4$.
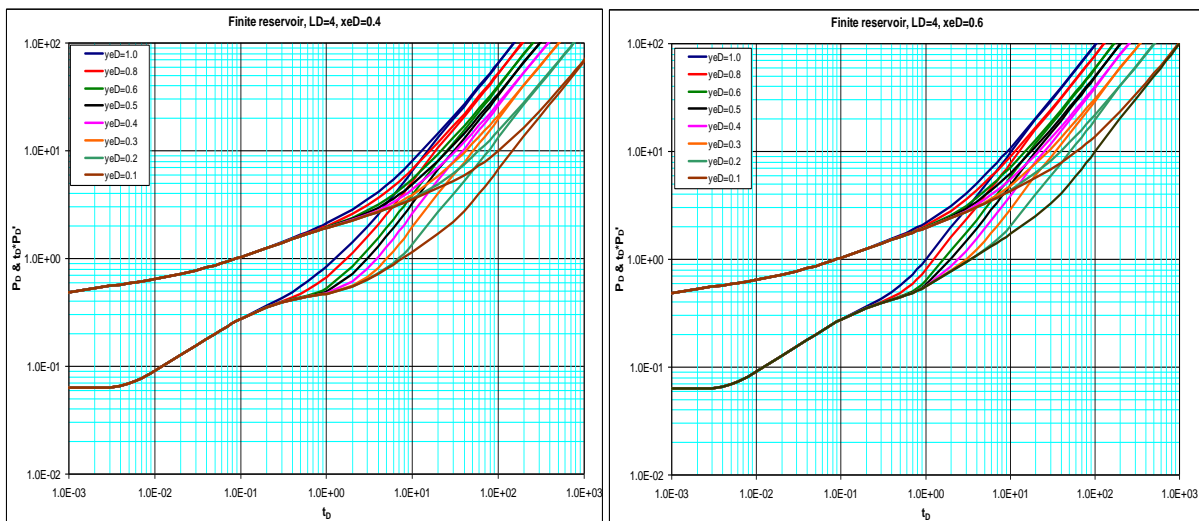
Fig. (A-9): Type curve for short horizontal well $L_D=4$.   Fig. (A-10): Type curve for short horizontal well $L_D=4$.
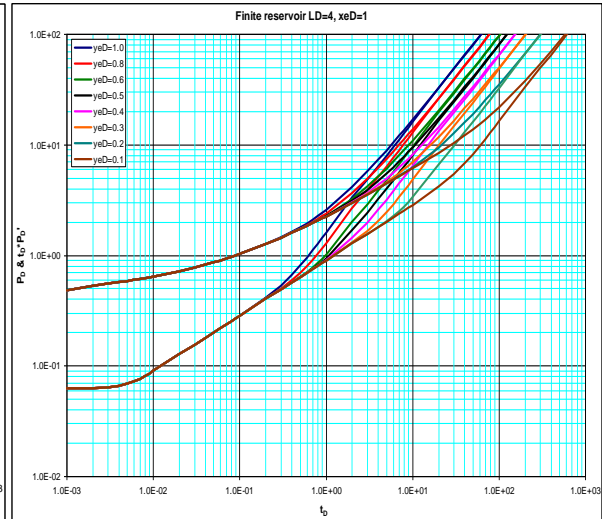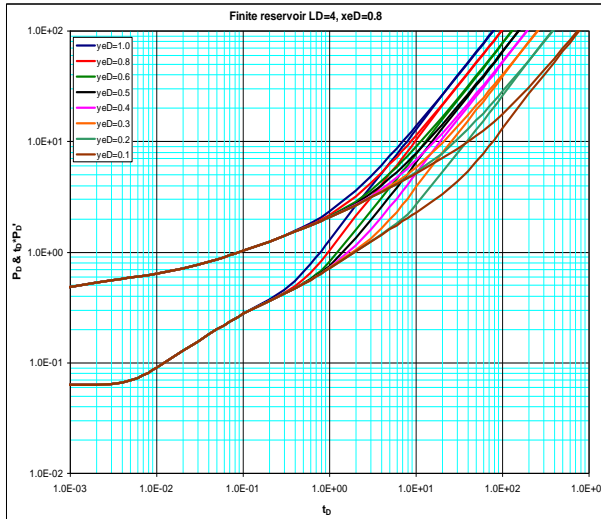
Fig. (A-11): Type curve for short horizontal well $L_D=4$. Fig. (A-12): Type curve for short horizontal well $L_D=4$.
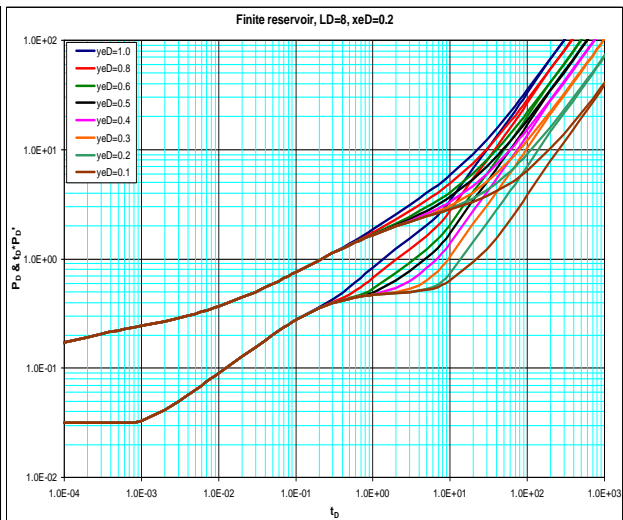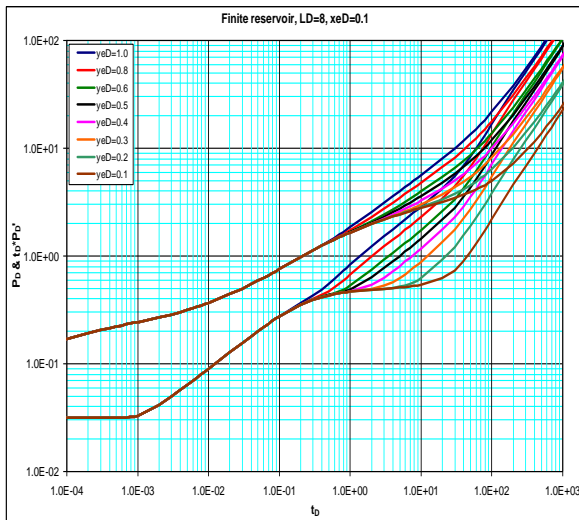
Fig. (A-13): Type curve for short horizontal well $L_D=8$. Fig. (A-14): Type curve for short horizontal well $L_D=8$.
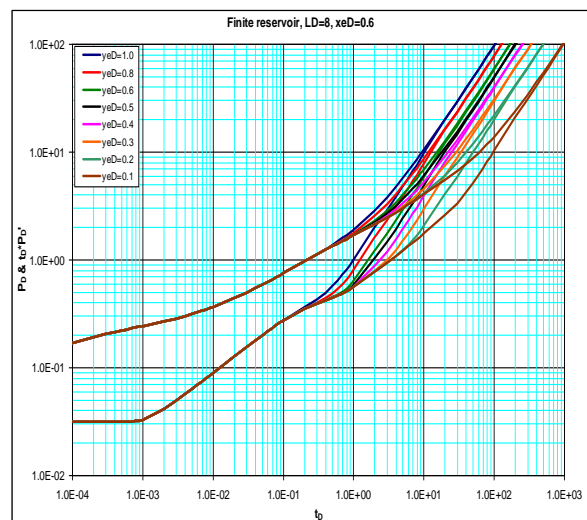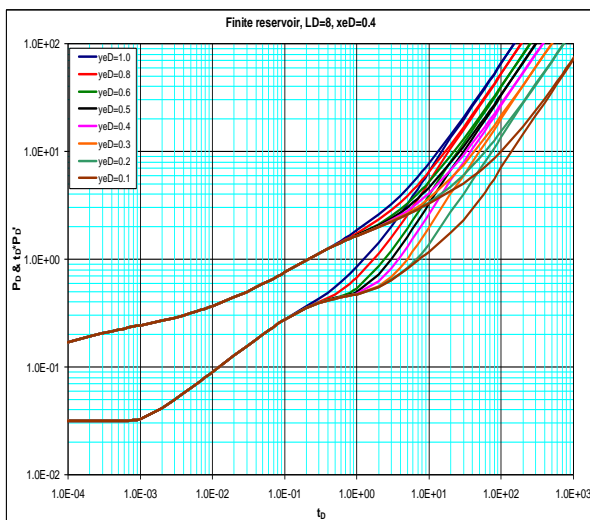
Fig. (A-15): Type curve for short horizontal well $L_D=8$. Fig. (A-16): Type curve for short horizontal well $L_D=8$.
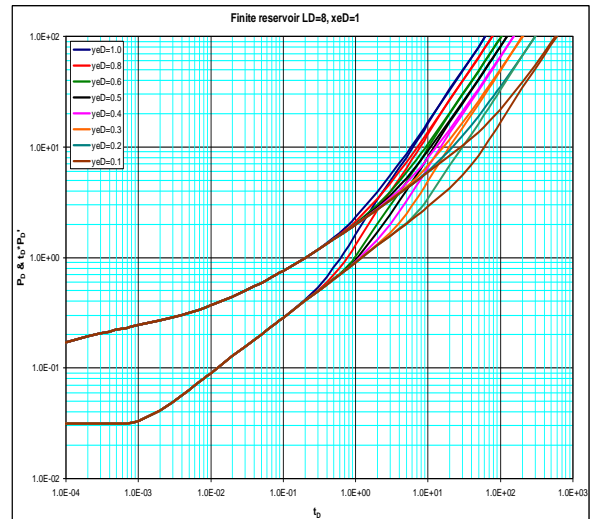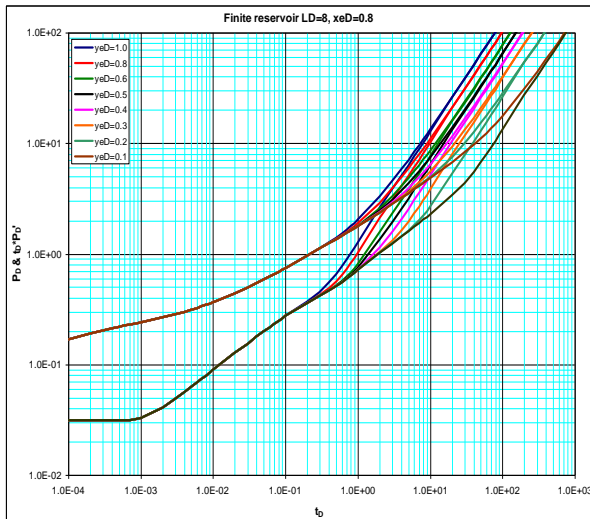
Fig. (A-17): Type curve for short horizontal well $L_D=8$. Fig. (A-18): Type curve for short horizontal well $L_D=8$.
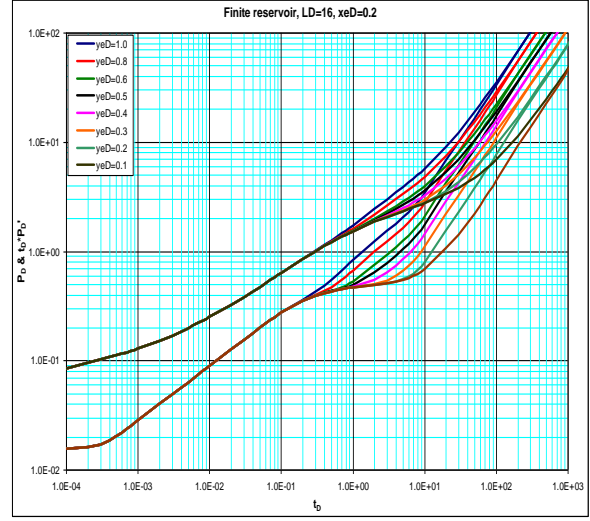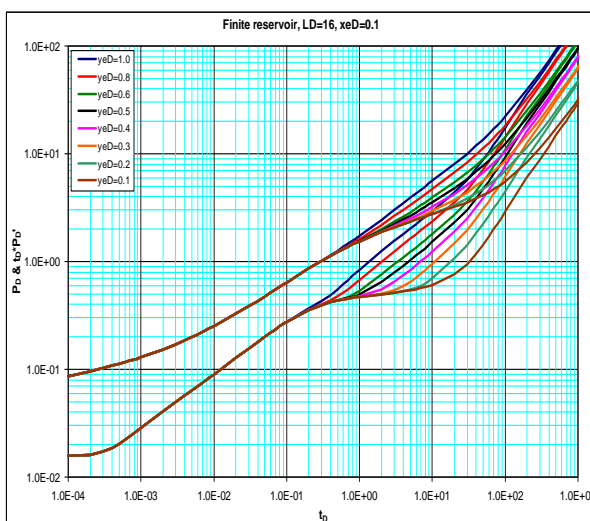
Fig. (A-19): Type curve for short horizontal well $L_D=16$. Fig. (A-20): Type curve for short horizontal well $L_D=16$.
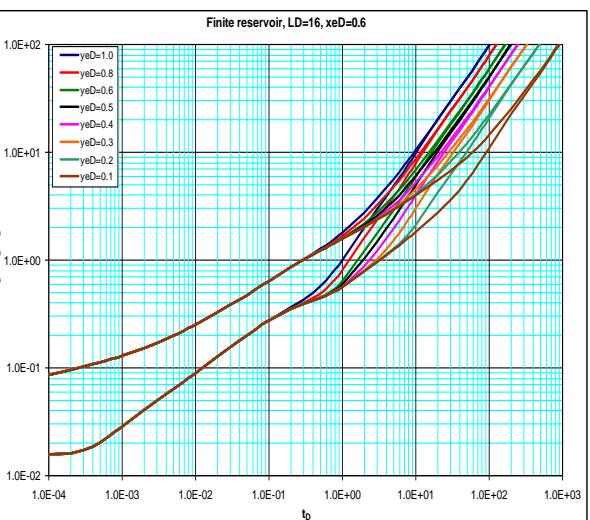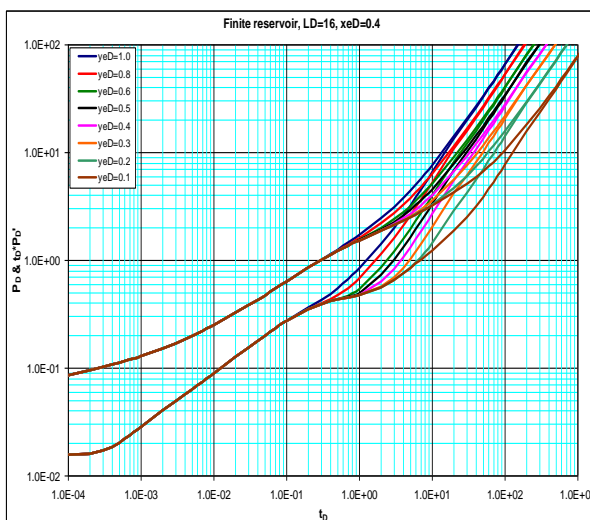
Fig. (A-21): Type curve for short horizontal well $L_D=16$. Fig. (A-22): Type curve for short horizontal well $L_D=16$.
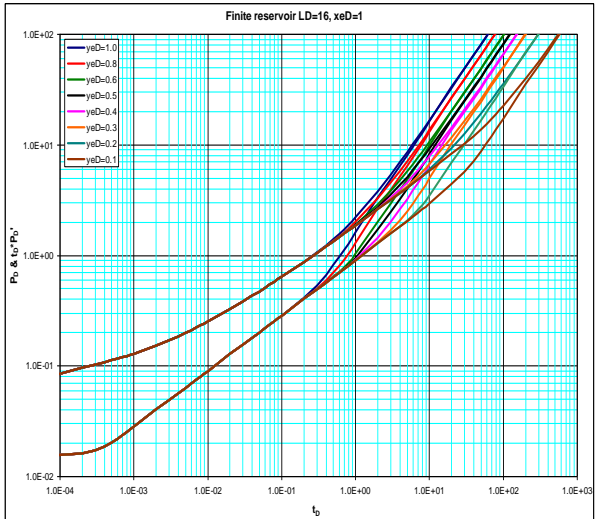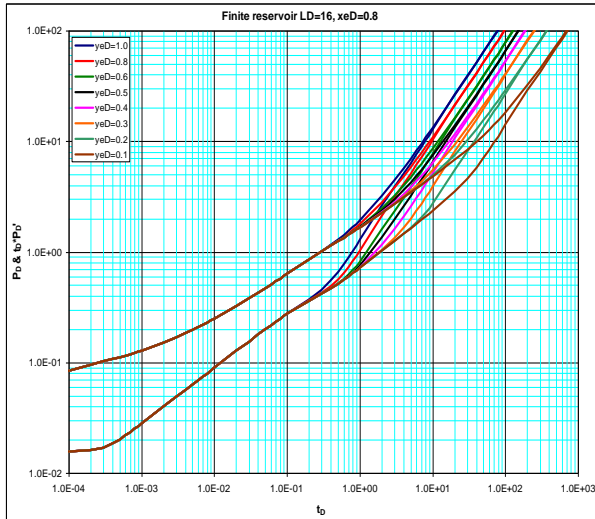
Fig. (A-23): Type curve for short horizontal well L_D=16. Fig. (A-24): Type curve for short horizontal well L_D=16.
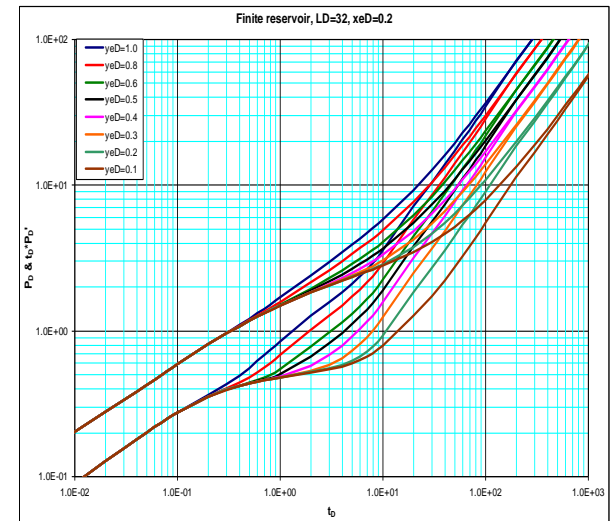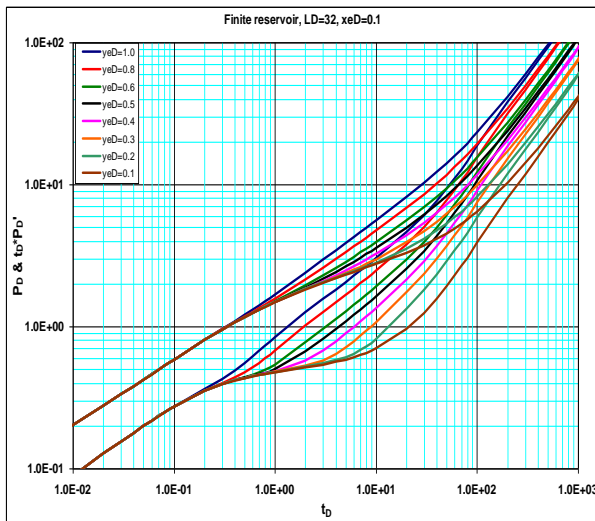
Fig. (A-25): Type curve for long horizontal well L_D=32. Fig. (A-26): Type curve for long horizontal well L_D=32.
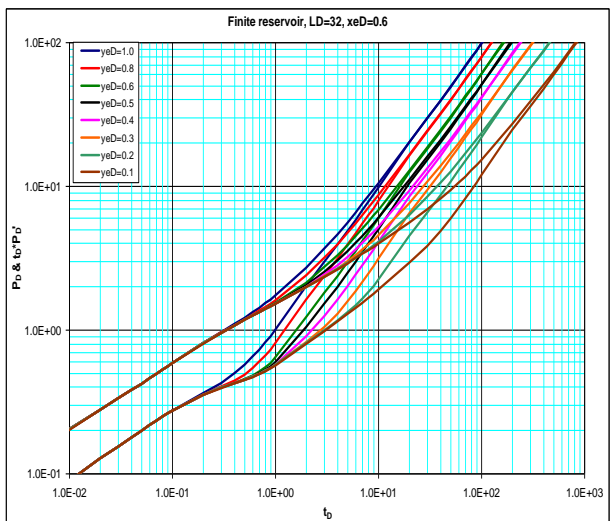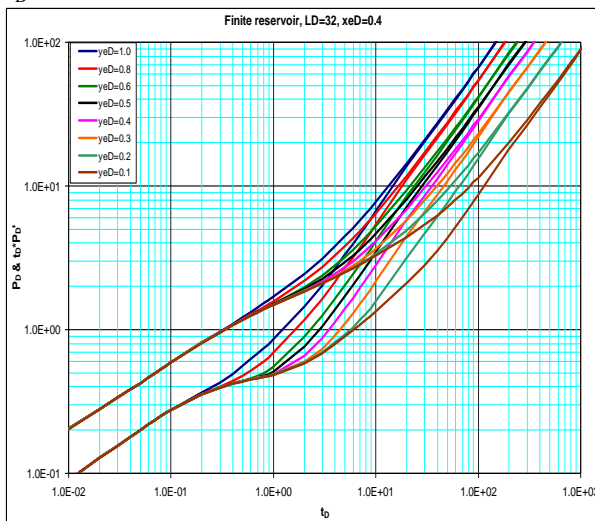
Fig. (A-27): Type curve for long horizontal well L_D=32. Fig. (A-28): Type curve for long horizontal well L_D=32.

Appendix B

Table B-1: Simulated Pressure Drawdown Data of Example.

t, hrs	Pwf, psi	t, hrs	Pwf, psi	t, hrs	Pwf, psi	t, hrs	Pwf, psi
0	9500	0.031533	9469.02	6.306661	9376.40	945.9992	8544.48
0.000315	9487.42	0.063067	9465.85	9.459992	9357.07	1261.332	8296.37
0.000631	9484.69	0.0946	9463.55	12.61332	9342.22	1576.665	8048.00
0.000946	9483.11	0.126133	9461.62	15.76665	9330.16	1891.998	7799.44
0.001261	9481.96	0.157667	9459.92	18.91998	9320.01	2207.331	7550.73
0.001577	9481.06	0.1892	9458.39	22.07331	9311.24	2522.665	7301.91
0.001892	9480.33	0.220733	9456.97	25.22665	9303.50	2837.998	7052.98
0.002207	9479.71	0.252266	9455.66	28.37998	9296.59	3153.331	6803.97
0.002523	9479.18	0.2838	9454.42	31.53331	9290.32	6306.661	4311.03
0.002838	9478.70	0.315333	9453.26	63.06661	9246.18	9459.992	1815.31
0.003153	9478.28	0.630666	9443.83	94.59992	9215.33		
0.006307	9475.50	0.945999	9436.59	126.1332	9188.42		
0.00946	9473.87	1.261332	9430.49	157.6665	9162.94		
0.012613	9472.72	1.576665	9425.12	189.1998	9137.99		
0.015767	9471.82	1.891998	9420.28	220.7331	9113.24		
0.01892	9471.09	2.207331	9415.83	252.2665	9088.56		
0.022073	9470.47	2.522665	9411.72	283.7998	9063.91		
0.025227	9469.94	2.837998	9407.87	315.3331	9039.25		
0.02838	9469.45	3.153331	9404.26	630.6661	8792.19		